Geophys. J. R. astr. Soc. (1971) **25,** 71–87.

The Propagation of Surface Waves in Anisotropic Media

Stuart Crampin and David B. Taylor

(Received 1971 January 21)

Summary

Surface wave propagation in examples of unlayered and multilayered anisotropic media is examined numerically with a programme using an extension of the Thompson–Haskell matrix formulation.

Surface wave propagation in an isotropic earth model containing an anisotropic layer in the upper mantle has been found, for the most part, to differ very little from propagation in a purely isotropic model. An exception is the propagation of the third generalized mode (corresponding to the second Rayleigh mode in isotropic structures), which has particle motion differing considerably from motion in isotropic media. Observations of such particle motion in the Earth have been made.

Introduction

The study of surface wave propagation in isotropic structures containing anisotropic layers is of importance to seismology in determining the presence or absence of anisotropic layers within the Earth. Most possible constituents of the Earth are anisotropic on a small scale, and mechanisms are present or have been present in the past, which could cause alignment of this anisotropy over wide areas, particularly in the upper mantle. This paper presents some numerical results of a programme, which uses the extension to anisotropic materials (Crampin 1970*) of the Thompson–Haskell matrix formulation, for calculating the dispersion characteristics of surface waves in multilayered media.

The object of this paper is to explore some examples of surface wave propagation in anisotropic media, and use these to interpret a possible geophysical structure. Surface waves in isotropic materials are degenerate forms of generalized surface wave propagation, and it is often not possible to interpret the behaviour in anisotropic media by analogy from the behaviour in isotropic media.

Analytical procedure

The matrix formulation (Crampin 1970) relates the six values of velocity and stress at the two interfaces of an isotropic or anisotropic plane-layer by a six-by-six matrix, whose elements can be evaluated numerically. The procedure then follows, in general outline, that suggested by Haskell (1953), although rather different in detail. The major differences arise from the need for complex arithmetic, and from modifications due to the three body waves which propagate in anisotropic media. The three body waves are a quasi-longitudinal wave and two quasi-transverse waves, propagating, in general, with different velocities and particle motions, which vary with direction in the material.

* This paper contains two copying errors: the line below equation (3.4) should read ' where for propagation in the x_1-direction $q_2 = 0$ ', and equation (6.3) should read.

$$' A^{-1} E(f(1), f(2), f(3), 0, 0, 0) = ((\dot{u}/c)_0, (\dot{W}/C)_0, 0, 0, (\dot{V}/C)_0, 0) '.$$

The velocities of the possible body waves contributing to the surface wave motion in each layer are obtained by substituting a plane wave $u_j = a_j \exp[i\omega(t - s_i x_i)]$ into the equations of motion for the layer. Eliminating the amplitude coefficients leads to the slowness equation, which is a sextic in s_1, s_2, and s_3. For any given apparent velocity and direction on the $x_1 x_2$ surface, s_1 and s_2 are determined and there are six roots of s_3 occurring in pairs with positive and negative imaginary parts. If we consider the x_3-axis positive into the material, the three roots with negative imaginary parts represent motion decreasing with depth.

The normal unattenuated modes of surface wave propagation have components from the three roots of the slowness equation with negative imaginary parts in the half space. Attenuated modes have components from at least one root with a positive imaginary part. In both layered and unlayered structures there may be a number of combinations of the six roots in the half-space, which satisfy the surface wave boundary conditions. In many cases there are combinations which yield solutions with small attenuation with distance. These are the pseudo or leaking modes which may be observed seismically and in model studies.

Numerical procedure

The programme searches for zeros of a complex determinant relating the boundary conditions at the free surface to those at depth. The velocity and frequency at which the determinant is zero are the conditions under which a surface wave can propagate. If we assume that the frequency is always real, normal mode roots are found along the real velocity axis for simultaneous zero crossing of both real and imaginary parts of the determinant. Leaking modes may, in most cases, be recognized by minima of the absolute determinant value along the real velocity axis. True zeros lie off the real axis in the direction of positive imaginary part. The minima of these pseudo roots on the real axis may be very narrow and easily escape notice. If the pseudo root is a long way from the real axis, or if the pseudo root otherwise does not produce a minimum on the real axis, more sophisticated and computer-time consuming techniques are required to detect the presence of the root.

Table 1

Crystal Parameters

Copper (cubic) $\rho = 8{\cdot}950$ g cm^{-3}
$c_{1111} = 171{\cdot}0$ $c_{1122} = 123{\cdot}0$ $c_{2323} = 75{\cdot}6\times10^9$ Newtons m^{-2}
orientation: (001) cut—direction measured from (100) angles.

Sapphire (trigonal) $\rho = 4{\cdot}00$ g cm^{-3}
$c_{1111} = 496{\cdot}8$ $c_{3333} = 498{\cdot}1$ $c_{1122} = 163{\cdot}6\times10^9$ Newtons m^{-2}
$c_{1133} = 110{\cdot}9$ $c_{1123} = -23{\cdot}5$ $c_{2323} = 147{\cdot}4$
orientation: (001) cut—direction measured from (100) angles.

Silicon (cubic) $\rho = 2{\cdot}332$ g cm^{-3}
$c_{1111} = 165{\cdot}7$ $c_{1122} = 63{\cdot}9$ $c_{2323} = 79{\cdot}56\times10^9$ Newtons m^{-2}
orientation: (111) cut—direction measured from (11$\bar{1}$) angles.

Zinc Oxide (hexagonal) $\rho = 5{\cdot}676$ g cm^{-3}
$c_{1111} = 209{\cdot}7$ $c_{3333} = 210{\cdot}9$ $c_{1122} = 121{\cdot}1\times10^9$ Newtons m^{-2}
$c_{1133} = 105{\cdot}1$ $c_{2323} = 42{\cdot}47$ $c_{1212} = 44{\cdot}29$
orientation: (001) cut—transversely isotropic in this plane.

Gold (isotropic) $\rho = 19{\cdot}3$ g cm^{-3}
$\lambda = 150{\cdot}05$ $\mu = 28{\cdot}5\times10^9$ Newtons m^{-2}

Olivine (orthorhombic) $\rho = 3{\cdot}324$ g cm^{-3} (Verma 1960)
$c_{1111} = 324{\cdot}0$ $c_{2222} = 198{\cdot}0$ $c_{3333} = 249{\cdot}0\times10^9$ Newtons m^{-2}
$c_{1122} = 59{\cdot}0$ $c_{2233} = 78{\cdot}0$ $c_{3311} = 79{\cdot}0$
$c_{1212} = 79{\cdot}3$ $c_{2323} = 66{\cdot}7$ $c_{1313} = 81{\cdot}0$
orientation: Fig. 6. (001), (100), (010) cuts—directions measured from (100), (010), and (001 angles, respectively. Figs 7–11. (001) cut—direction measured from (100) angles.

Positive directions are parallel to an interface or downwards. Changes of orientation are measured in a clockwise direction viewed from above.

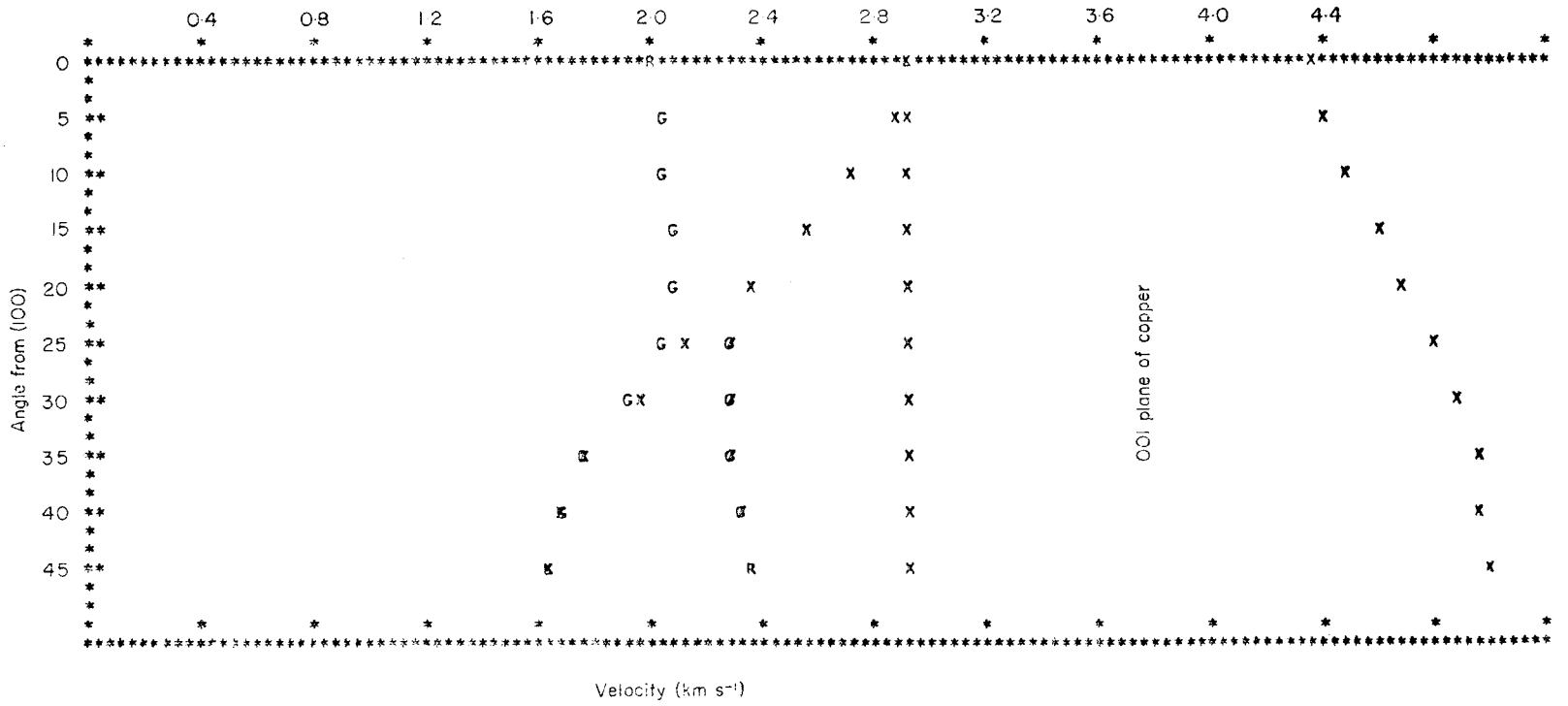

FIG. 1. Lineprinter plot of wave velocities in a copper half-space (elastic constants and orientations are given in Table 1). " X " represents body waves propagating parallel to the interface, " G " generalized surface waves, " R " Rayleigh-type motion, and " L " Love-type motion. A superimposed solidus represents leaking propagation.

The system of matrices giving the determinant must be completely re-calculated for every new trial velocity, whereas at a fixed velocity, new frequency trials alter each matrix by a simple diagonal multiplier. Thus, it may take less time to find the frequencies at which several modes travel at one velocity in a multilayered structure, than it does to find the velocity at which a surface wave propagates in a homogeneous half-space.

Fig. 1 is a lineprinter output giving the wave velocities for a range of directions on the (001) plane of copper (the elastic constants of all materials are listed in Table 1). For each direction, there are three-body waves parallel to the surface, and a generalized surface wave. Rayleigh- and Love-type propagation is present along directions of symmetry. Some of these waves are attenuated, and are marked by a superimposed solidus. This calculation took about 4 min of IBM 360/50 time.

Each velocity curve in Fig. 1 is a segment of a plane section of the slowness surface for that mode of propagation. It has been found that three-dimensional models of the slowness surfaces of each of the wave types in a particular material are a considerable aid in understanding the behaviour of the waves as the material is rotated.

Group velocity

The procedure we have outlined yields the phase velocity; that is the velocity perpendicular to the wave front. In anisotropic media there is a component of energy propagating parallel to the wave front, and, except in directions of anisotropic symmetry, the group velocity cannot be found by differentiating the phase velocity, as is the case in isotropic media. The energy propagates in a straight line from the source in the absence of a vertical discontinuity, and the phase velocity direction will show convolutions about this straight line.

It may be shown by a simple extension of Sommerfeld's method (Richter 1958) that the longitudinal and transverse components of the group velocity of an unattenuated surface wave are $\partial\omega/\partial\alpha$, $\partial\omega/\partial\beta$, where ω is the angular frequency, and α and β are the wave numbers parallel to the propagation vector, and the wave front, respectively. In isotropic structures, where for a given frequency there is no variation of wave number with directions, the wave numbers α and β are inversely proportional to the direction cosines, and the expression for the group velocity can be written in the familiar $\partial\omega/\partial\kappa$, where κ is the wave number in the direction of the propagation vector.

By partial differentiation of $\omega(\alpha, \beta)$, we have

$$\Delta\omega = \frac{\partial\omega}{\partial\alpha}\Delta\alpha + \frac{\partial\omega}{\partial\beta}\Delta\beta, \tag{1}$$

where $\Delta\omega$, $\Delta\alpha$, and $\Delta\beta$ are small increments in ω, α, and β, respectively. $\partial\omega/\partial\alpha$ is the group velocity resolved perpendicular to the wave front and can be determined by differentiation of the phase velocity. $\Delta\omega$, $\Delta\alpha$, and $\Delta\beta$ can be obtained by calculating the dispersion after having made an infinitesimally small change in direction of propagation on the structure. Substituting these values into (1), we have $\partial\omega/\partial\beta$, the component of the group velocity parallel to the wave front. The values of $\partial\omega/\partial\alpha$ and $\partial\omega/\partial\beta$ together determine the group velocity magnitude and direction.

The procedure outlined above provides a way of determining the velocity and direction of energy propagation at any point on a wave front of a normal mode travelling in a given direction. The problem more pertinent to seismology of calculating the velocity at which energy travels in a given direction, and the inclination of the wave front to this direction, requires a trial and error technique. It necessitates calculating the phase velocity dispersion in neighbouring directions until one has found the group velocity in the required direction. This can be done for the non-dispersed case of propagation on an homogeneous half-space, where the variation of

the group velocity is usually smooth, but finding the group velocity dispersion in a straight line on a layered structure requires considerable additional computation and this has not been attempted.

In general, the variation of the phase velocity with material orientation, in both multilayered and unlayered half-spaces, is insufficient to make $\partial\omega/\partial\beta$ very large, and the inclinations of the group and phase velocities will differ by only a few degrees and the absolute values by a few percent (see for example Figs 2, 6 and 10). However, it cannot be excluded that the group velocity direction, on some sections of higher mode dispersion in particular multilayered cases, might differ considerably from the phase velocity direction.

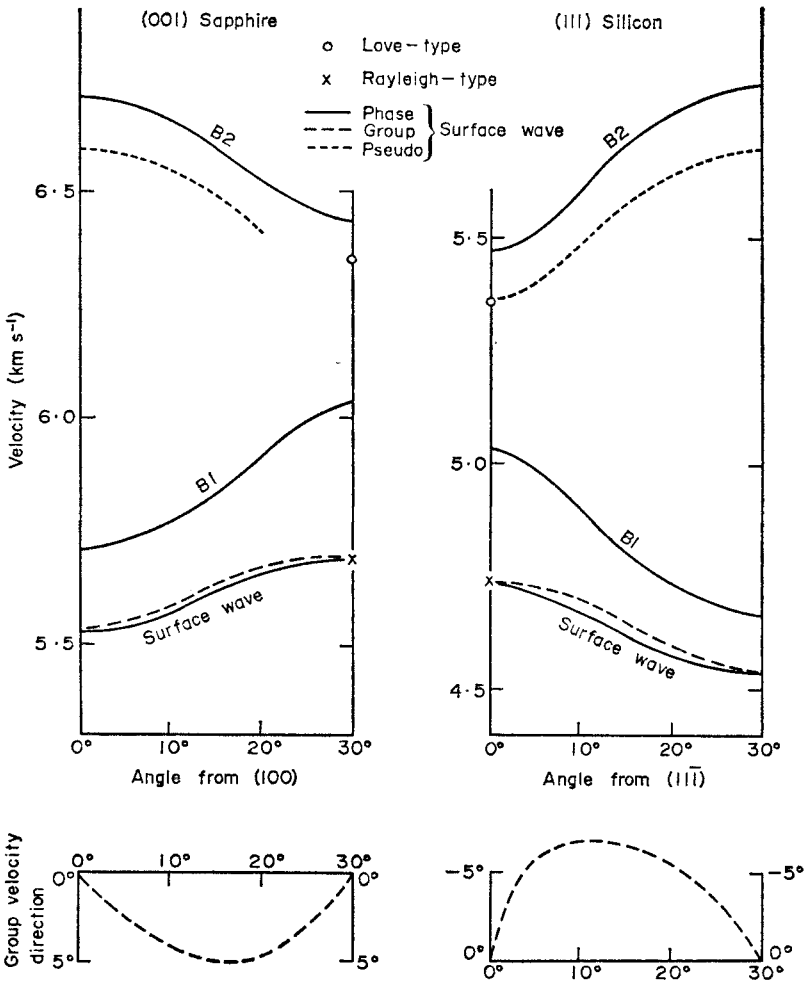

FIG. 2. Wave velocities in sapphire and silicon half-spaces (see Table 1). The quasi-transverse body waves propagating parallel to the interface are labelled B1 and B2. The quasi-longitudinal body waves are not shown.
The group-velocity magnitude and direction is shown at the orientation of the phase velocity propagation. The inclination of the group velocity to the phase velocity is measured in a clockwise direction viewed from above.

Examples of propagation in anisotropic structures

The propagation characteristics of surface waves on a variety of anisotropic structures have been calculated in order to gain some understanding of surface wave behaviour under anisotropic conditions. As an illustration, Figs 2–5 show the velocities of surface waves in various structures made up of gold, on zinc oxide, on silicon, on a sapphire half-space. The elastic constants and details of the structures are given in Tables 1 and 2. The orientations have been chosen so that there is no overall direction of anisotropic symmetry. The dimensions of the models used for Figs 3–5 are appropriate for experimental models.

Fig. 2 shows wave propagation in half-spaces of sapphire (trigonal), and silicon (cubic) with the free surface along the (001), and (111) cuts, respectively. The quasi-longitudinal wave velocities are not shown. In both cases, the wave velocities are symmetrical in directions at every 30°. The condition for symmetry of the body wave velocities is a weaker condition than that for full elastic symmetry, which occurs in directions at every 60° in these materials. In directions of elastic symmetry, when the free surface is also a plane of symmetry, the surface wave equation factorizes (Crampin 1970), and represents two independent waves propagating with Rayleigh- and Love-type particle motion. Figs 1 and 2, show such motion along directions of elastic symmetry.

Fig. 2 also shows the group velocity of the generalized surface wave for any given direction of the propagation vector, and its inclination to the propagation vector. In unlayered half-spaces the group velocity of the generalized wave is greater than or equal to the phase velocity. Both half-spaces in Fig. 2 allow pseudo or leaking waves

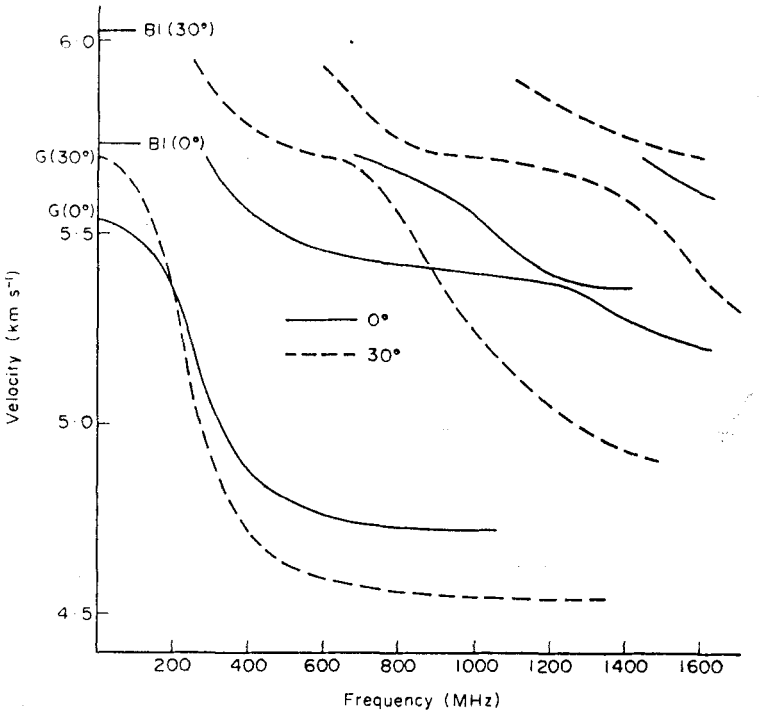

FIG. 3. Phase velocity dispersion of the first four generalized normal mode surface waves propagating in two directions in 10μ of silicon overlying a sapphire half-space (see Tables 1 and 2). B1 are the lowest velocities of body waves propagating parallel to the interface, and ' G ' are the generalized surface wave velocities in the half-space, at the appropriate orientations.

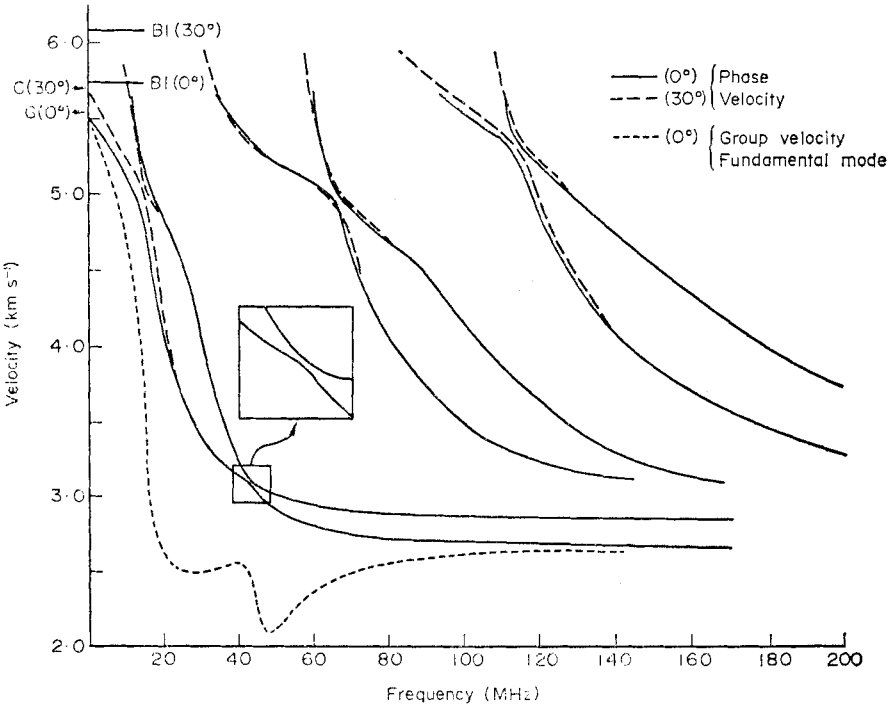

FIG. 4. Phase velocity dispersion of the first six generalized normal mode surface waves propagating in two directions in 30μ of zinc oxide, on 10μ silicon, overlying a sapphire half-space (see Tables 1 and 2). Group velocity is shown for the fundamental mode in the 0° direction.

to propagate. It became increasingly difficult to follow the pseudo root in sapphire as it approached the Love-type root on the direction of symmetry: the imaginary part of the velocity became very small, and the minimum was very steep sided and narrow.

There is very little velocity contrast between the lowest quasi-transverse wave of sapphire and the highest quasi-transverse wave of silicon. The closeness of these two velocities, result in some rapid changes in the dispersion curves of Fig. 3, which shows the first four normal mode surface waves propagating in a structure consisting of a layer of silicon on a half-space of sapphire. The dispersion curves are given at 0° and 30° from the orientations listed in Table 1. The fundamental modes tend to the surface wave velocity in the half-space as the frequency decreases. The higher modes have a high-velocity, low-frequency cut-off at the lowest quasi-transverse body-wave velocity in the half-space propagating parallel to the interface.

A characteristic feature of dispersion in layered anisotropic structures is the pinching together of two modes, here the second and third modes. Each mode is a combination of the three body waves. In the half-space, there is one component from each body wave, and in a layer, there is a pair of components from each body wave—one travelling towards and one away from the surface. Generally, the particle motion of the two quasi-transverse body waves is perpendicular (the particle motions of the three body waves are mutually orthogonal). Typically, successive modes of surface waves have their largest transverse components in each strata from alternate transverse body waves, and they alternate in the size of their quasi-longitudinal components. The pinching together represents places where two adjacent modes interchange their relative holdings of each body wave, either in the half-space or in one of the layers. In structures where there is a direction of symmetry, as the propagation

Table 2

Structural models

Fig. 3	10μ silicon, on sapphire half-space			
Fig. 4	30μ zinc oxide, on 10μ silicon, on sapphire half-space.			
Fig. 5	2μ gold on 30μ zinc oxide on 10μ silicon on sapphire half-space			
Fig. 7	h	ρ	α	β
	10 km	2·7	5·8	3·4
	20 km	2·9	6·6	3·8
		3·324	olivine half-space (see Table 1).	
Figs 8–11	h	ρ	α	β
	10 km	2·7	5·8	3·4
	20 km	2·9	6·6	3·8
	30 km	3·324	olivine layer	
		3·6	9·0	5·4

Composite models are made up with the orientations given in Table 1.

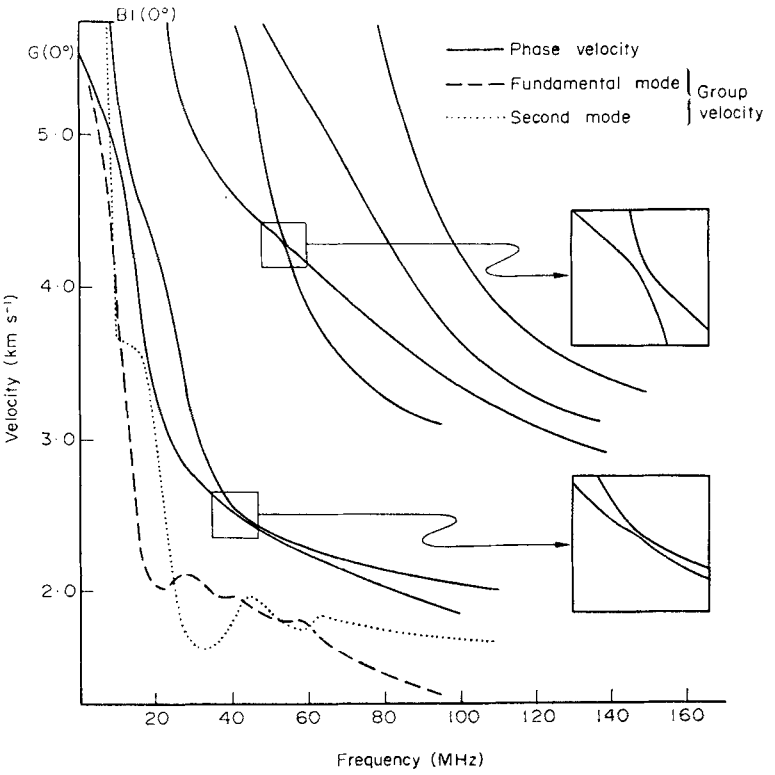

FIG. 5. Phase velocity dispersion of the first six generalized normal mode surface waves propagating in the 0° direction in 2μ of gold, on 30μ of zinc oxide, on 10μ of silicon, overlying a sapphire half-space (see Tables 1 and 2). Group velocity is drawn for the first and second modes.

approaches this direction, a pinch becomes a place where the Rayleigh- and Love-type dispersion curves cross each other. Thus the pinches are some measure of the nearness of the elastic parameters to symmetry about the particular propagation direction, at the depths to which the motion of the pinched modes penetrates. The pinch in the 0° direction in Fig. 3 is tighter than the pinch in the 30° direction, because most of the energy propagates near the surface, and the surface layer is symmetric about the 0° direction.

Fig. 4 shows the first six normal modes in directions 0° and 30° in a structure consisting of a layer of zinc oxide overlying the previous model (see Tables 1 and 2). The layer of zinc oxide is transversely isotropic for the given orientation, and the dispersion of the modes changes with direction only at lower frequencies, where a larger proportion of the energy travels beneath the upper layer in the more anisotropic deeper structures. The major differences with changes in direction, are the variation of the high-velocity, low-frequency cut-off at the body-wave velocities parallel to the interface in the half-space. Group velocities are drawn for some of the modes in Figs 4 and 5 to show the rapid variations to be expected when the phase velocity is near a pinch.

Fig. 5 shows the first six normal modes in the 0° direction in a structure consisting of a thin layer of isotropic gold overlying the previous model. The computer program produced the general outline of this figure in eight minutes of IBM 360/50 time (the first six zero crossings at 20 given velocities). Computing the behaviour of the dispersion in the neighbourhood of the pinches, which are extremely tight for this structure, took additional computing time.

Examples of propagation in earth models with anisotropy in the upper mantle

The remainder of the paper discusses the propagation of surface waves in an isotropic crust overlying (a) an olivine mantle, and (b) an isotropic mantle with a layer of olivine beneath the crust (see Tables 1 and 2). The olivine is taken to be crystalline with complete alignment. We shall first examine the propagation of surface waves in a homogeneous olivine half-space.

Olivine half-space

Olivine is orthorhombic and for propagation in media with orthorhombic symmetry, the two quasi-transverse body waves, propagating parallel to the surface, where one of the planes of symmetry is parallel to the free surface, are approximately quasi-SH and quasi-SV. These we shall label QSH and QSV, respectively. However, except along directions of symmetry, each wave has particle motion containing SH, SV and longitudinal components. Fig. 6 shows wave velocities for different directions on the three planes of symmetry of olivine. The quasi-longitudinal body waves have velocities between 7·7 and 9·9 km s^{-1} and are not shown. Pseudo waves were found only on the (100) cut. In this plane, the generalized surface wave continues the line of the pseudo wave, where the pseudo wave meets the quasi-SH body wave. At this point, the line of the generalized wave bends sharply, and follows the body wave to the direction of symmetry.

The Rayleigh-type motion marked on the directions of symmetry are at the positions calculated by Stoneley (1963). The Rayleigh-type motion is on the continuation of the generalized surface wave for propagation on the (001) and (010) planes. On the (100) plane however, the Rayleigh-type motion is on the continuation of the pseudo wave, whose attenuation decreases until it is zero at the Rayleigh wave on the direction of symmetry. Thus although it is impossible for a generalized normal surface mode to propagate in an isolated direction on a crystal surface (Burridge 1970), it is possible for unattenuated Rayleigh-type waves to propagate in isolated directions.

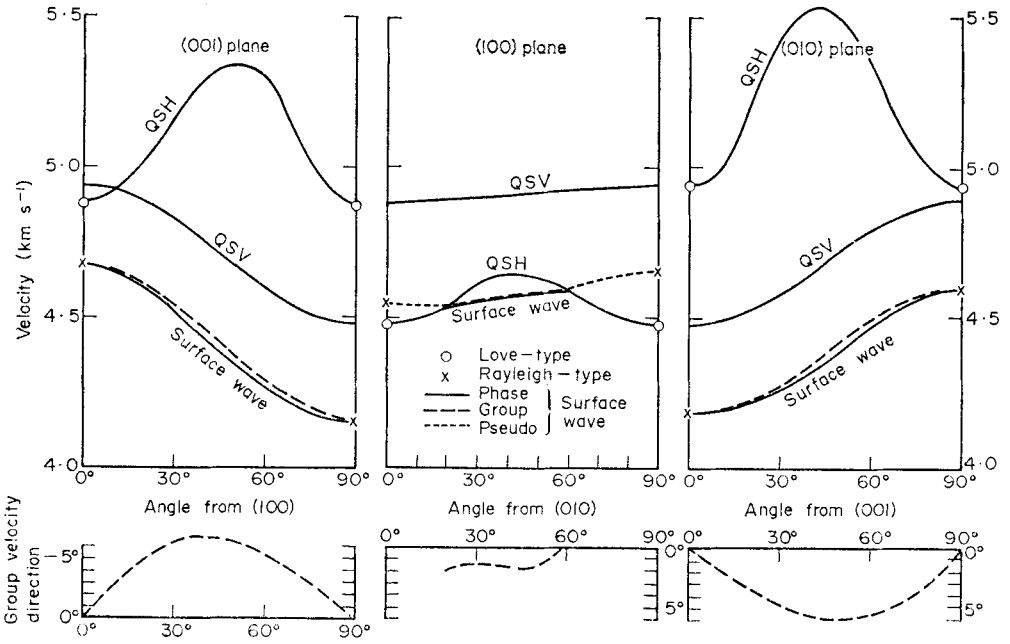

FIG. 6. Wave velocities in olivine half-spaces with each of the three planes of symmetry aligned parallel to the free surface (see Table 1).

Isotropic crust overlying olivine mantle

Fig. 7 shows the first four normal modes in four directions on a structure consisting of two isotropic layers, totalling 30 km in thickness, over an olivine half-space with the (001) cut as the interface (see Tables 1 and 2). Along directions of symmetry at 0° and 90°, the odd numbered generalized modes have Rayleigh-type particle motion in the sagittal plane, and the even modes have Love-type particle motion in the transverse horizontal plane. We see that the two distinct families of Rayleigh and Love modes in isotropic media are subsets of a family of degenerate generalized modes.

The fundamental mode in Fig. 7 tends to the surface wave velocity in the half-space at long periods, and its general behaviour as the direction of propagation was varied could be predicted from the variation of the half-space velocity in the previous figure. The higher modes have velocities less than the lowest body wave velocity parallel to the interface, although there are leaking mode extensions into higher velocities. The odd modes, which have Rayleigh-type motion in symmetry directions, have their largest contributions from the quasi-longitudinal and QSV body waves, although there is a small contribution from QSH. The even modes have their largest contribution from the QSH body wave. (Behaviour of the even and odd modes is modified by the pinching that occurs between the higher modes). Thus, as the direction of propagation varies, the even modes rise and fall with the variation of the QSH body wave, and the third and higher modes rise and fall with the QSV body wave.

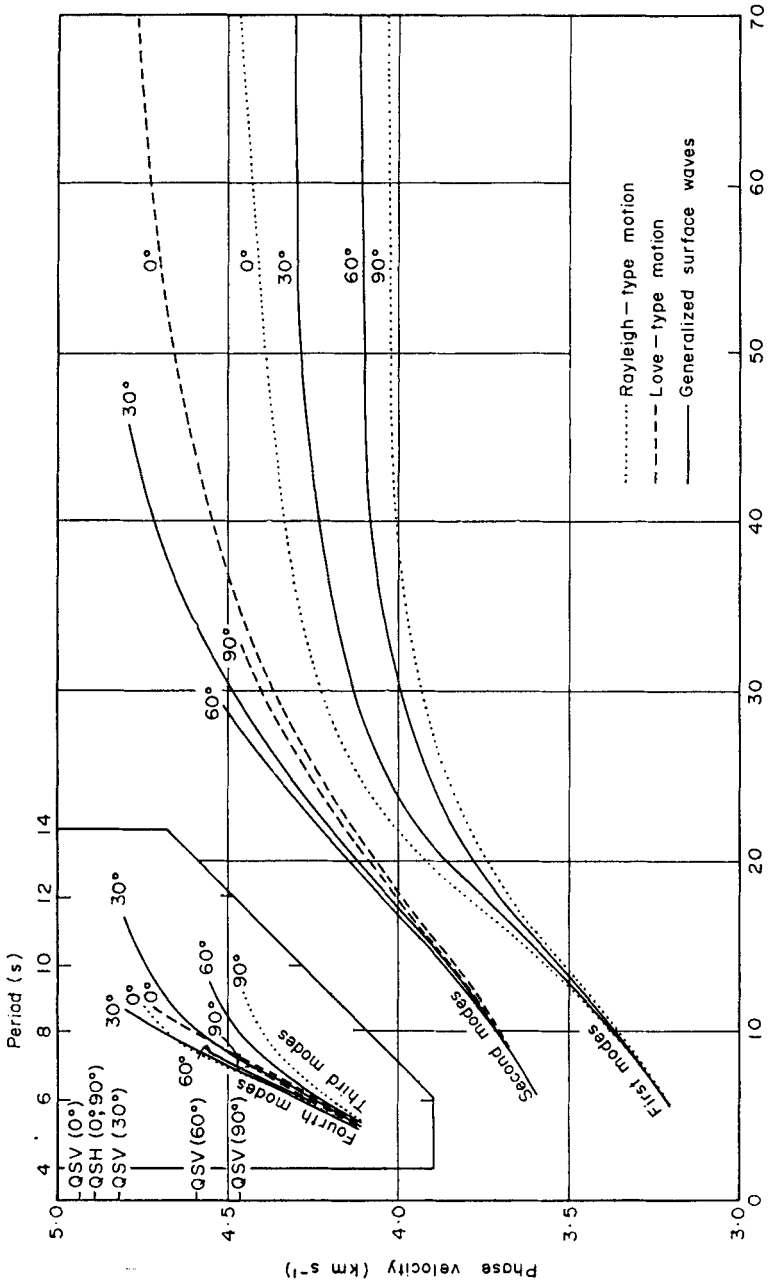

FIG. 7. Phase velocity dispersion of the first four generalized normal mode surface waves propagating in four directions on two isotropic layers overlying an anisotropic olivine half-space (see Tables 1 and 2).

Isotropic crust overlying an isotropic mantle with an olivine layer in the upper mantle

Fig. 8 shows the phase velocity of the first four normal modes in four directions on a structure consisting of two isotropic layers, totalling 30 km in thickness, over a 30 km layer of olivine, overlying an isotropic half-space (see Tables 1 and 2). The velocities in the half-space were chosen so that unattenuated normal modes would propagate in all directions.

The variation of the dispersion curves with changes of propagation direction is similar to that in the previous model, with the exception that the first and second modes show less variation with direction, particularly at longer periods, where a larger proportion of the energy travels in the isotropic half-space.

Fig. 9 shows the group velocity dispersion corresponding to the phase dispersion given in Fig. 8. The group and phase velocities are parallel for propagation in the directions of symmetry at 0° and 90°. The other group velocities shown are inclined to the propagation vectors at 30° and 60° by the period dependent angles in Fig. 10, which are positive in a clockwise direction viewed from above. These group velocity angles are all less than 5° for the modes examined, and the difference between the group velocity (given in Fig. 9) and its resolution along the propagation vector is less than 1 per cent.

The layer of olivine has been aligned so that the (001) plane of symmetry is parallel to the free surface. It can be shown by an extension of the method used in Section 6 of Crampin (1970) that the generalized surface waves have elliptical particle motion in a vertical plane inclined to the direction of propagation, when propagating on structures made up of strata having planes of symmetry parallel to the free surface. In directions of crystal symmetry on these planes, the surface waves separate into Rayleigh- and Love-type modes with the more familiar particle motion of Rayleigh and Love waves in isotropic media. Fig. 11 shows the inclination of the plane containing elliptical particle motion at the surface to the propagation vector. The inclinations have been drawn, along propagation directions of 30° and 60°, for retrograde elliptical motion—subtraction of 180° would give the inclination of prograde motion. The inclinations have different scales in different sections of the figure.

In Fig. 11, the first generalized mode, which yields the fundamental Rayleigh mode along directions of symmetry, has its largest divergence from the sagittal plane between periods of 20 and 30 s, where the maximum inclination is some 15°. The first mode has more energy travelling in the anisotropic layer at these periods than at other periods.

The second and fourth modes, which yield Love-type motion along directions of symmetry, have small vertical components of motion, and the inclination is only a few degrees away from pure transverse motion. In each of these modes there is one point on the dispersion curve where the small vertical component at the surface changes sign and passes through a zero. This introduces a 180° change in the inclination of the the retrograde motion. For plotting convenience, the inclination of prograde motion has been continued after the sign change as a dashed line.

The variation of the amplitude with depth of the third mode (analogous to the second Rayleigh mode of propagation in isotropic media), has one node. Typically, the lower lobe of motion has much greater amplitude than the lobe near the surface. In the structure from which Fig. 11 is derived, the third mode has the large lower lobe propagating in and around the layer of anisotropic olivine; thus the third modes have a large range of inclinations. This large range has been observed in seismology. The fourth modes have three lobes of amplitude with depth, but in this structure there is no one major lobe in the anisotropic layer.

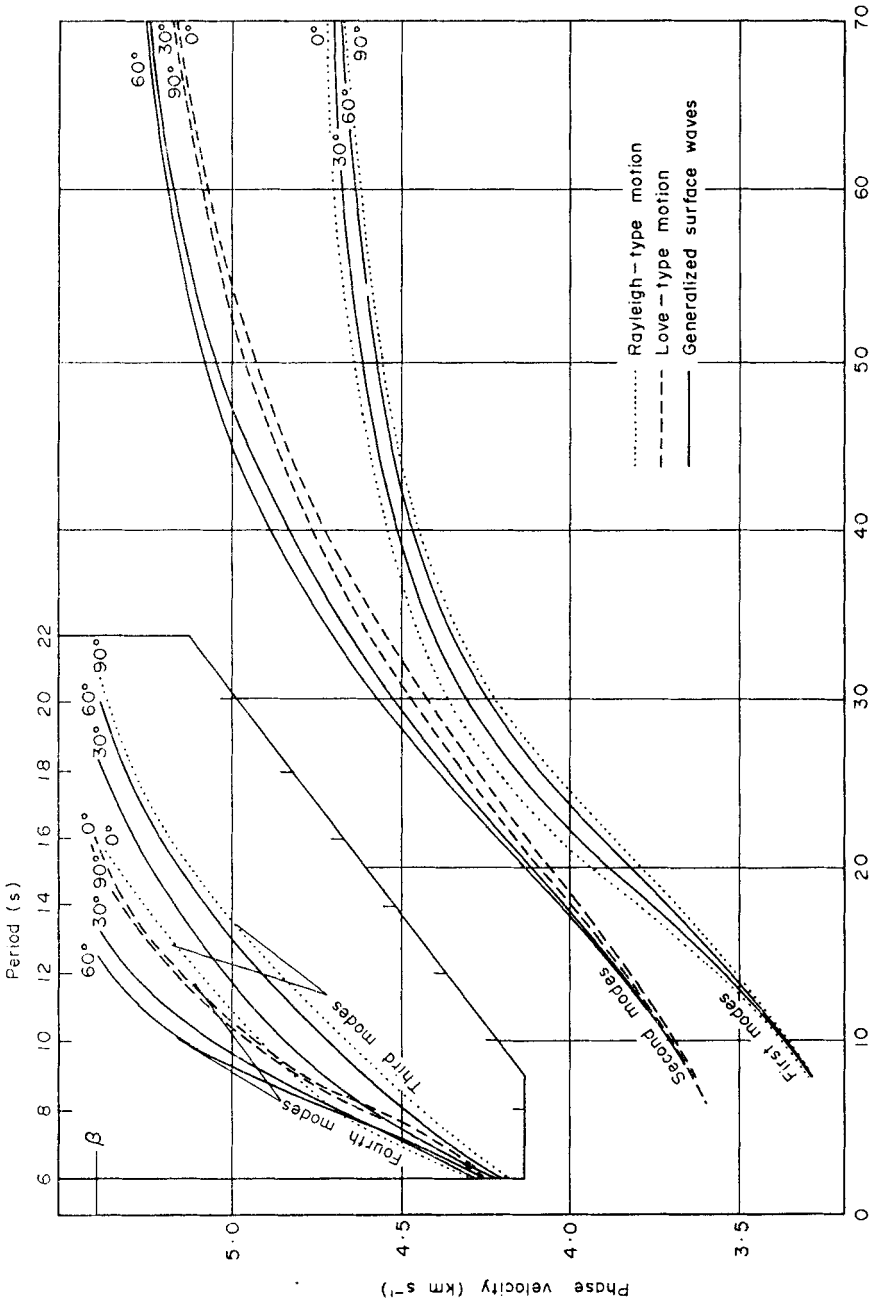

FIG. 8. Phase velocity dispersion of the first four generalized normal mode surface waves propagating in four directions on a structure consisting of two isotropic layers, over an olivine layer, overlying an isotropic half-space. β marks the shear wave

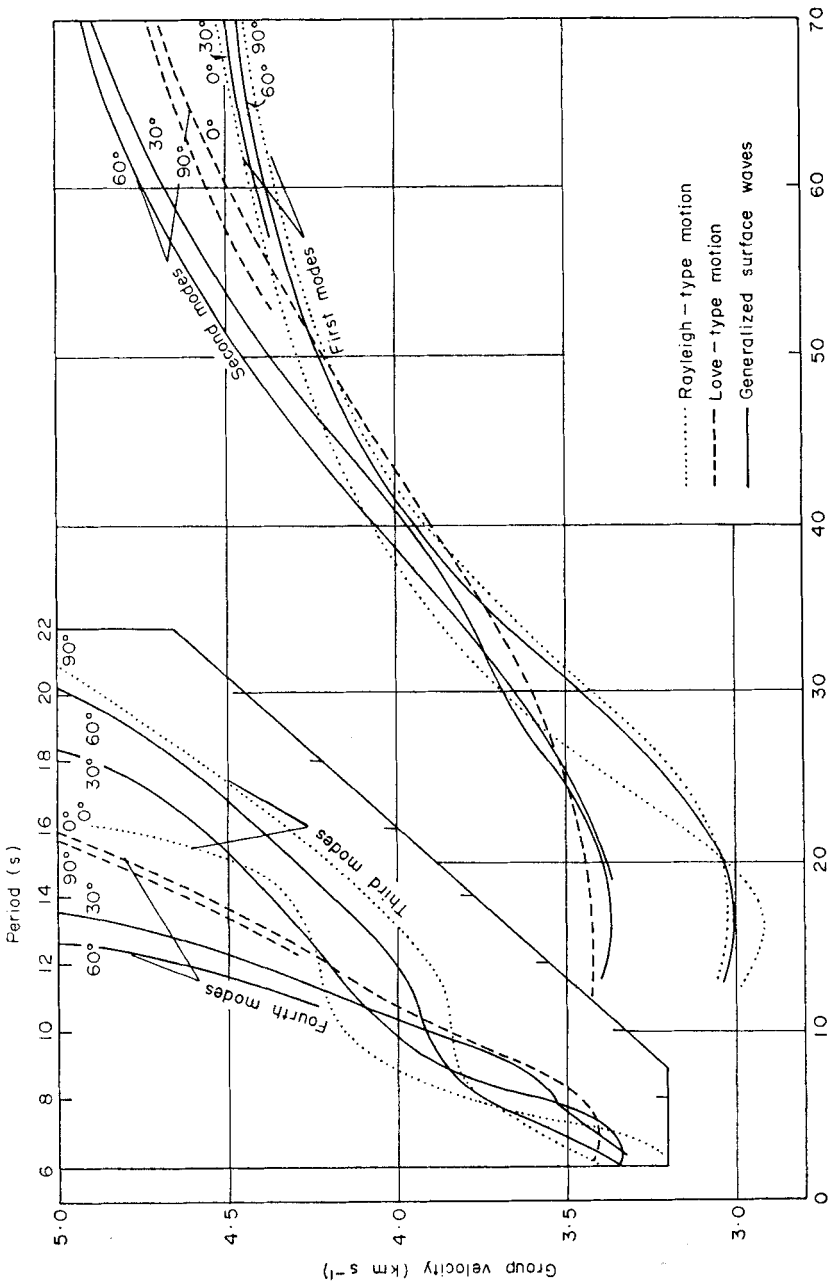

FIG. 9. Group velocity dispersion corresponding to the phase velocities in Fig. 8. In directions 30° and 60° the group velocities are approximate.

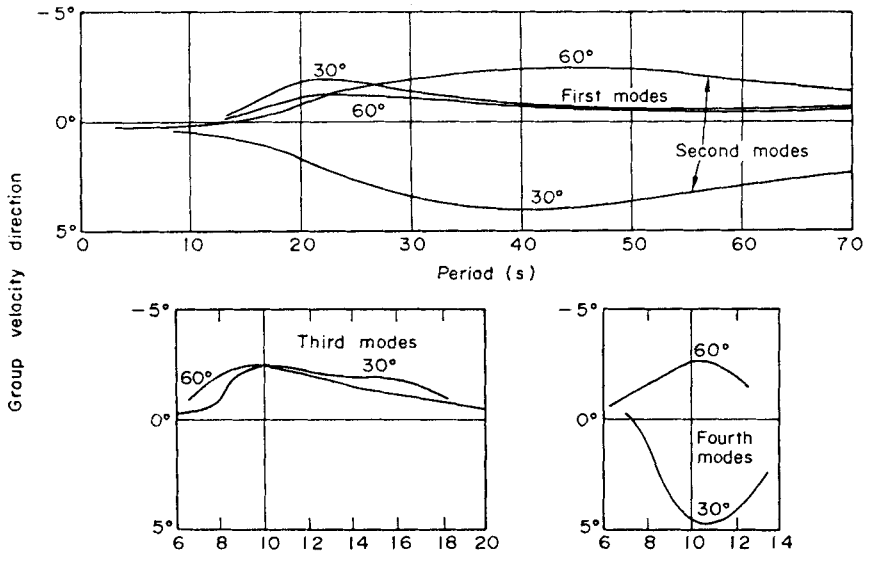

FIG. 10. Inclination of the group velocity in Fig. 9 to the propagation vector for propagation directions of 30° and 60°.

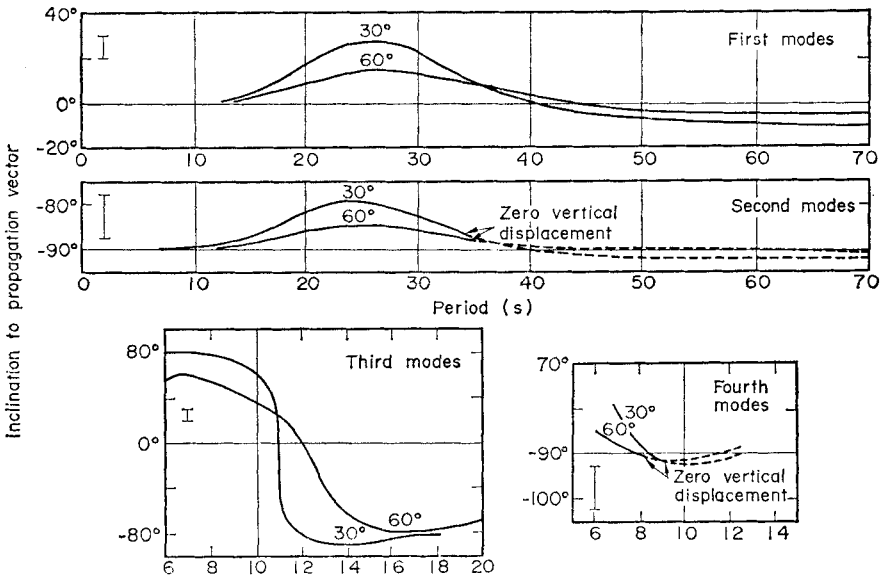

FIG. 11. Inclination of horizontal particle motion at the surface to the propagation vector corresponding to phase velocities of Fig. 8. The inclination is measured in a clockwise direction viewed from above. The bar on the left of each figure, gives the measure of an inclination of 10° in the appropriate scale.

Geophysical discussion

The most probable place where aligned anisotropy occurs in the Earth on a sufficiently large scale to modify surface waves is the upper mantle. In the upper mantle crystalline structures could be aligned by the stresses associated with convection currents or with plate tectonics.

The structure used for Figs 8–11 is not a realistic earth model. The layer of olivine and the half space have velocities which do not agree with seismic travel times. A more realistic model might be contrived using constituents other than olivine, by using cuts of olivine where the velocities are lower (such as the (100) plane, see Fig. 6), or by using olivine where only a percentage of the crystals are aligned with the same orientation. However, the structure is a first approximation and may give some indication of the effects of an anisotropic upper mantle on surface wave propagation.

The majority of the effects are second-order variations of isotropic propagation. Observations of these phenomena would be difficult to separate from similar effects due to changes in layering, vertical discontinuities, and other inhomogeneities of an isotropic earth.

As stresses in the upper mantle are in general either perpendicular or parallel to the surface, it is reasonable to suppose that any aligned anisotropy present would have a horizontal plane of symmetry. Thus, in the presence of anisotropy, we might expect the fundamental Rayleigh waves (first generalized mode) to have elliptical particle motion in a vertical plane inclined to the direction of propagation. In addition, if there is anisotropy with any alignment present, the fundamental Love waves (second generalized mode) would have a vertical component of particle motion. Both these phenomena have been observed. The Rayleigh waves have usually been interpreted as isotropic waves arriving from non great-circle path.

One feature is markedly different in Fig. 11 from that of surface waves propagating on a similar isotropic model. This is the particle motion of the second Rayleigh waves (third generalized mode), which is elliptical in a vertical plane inclined to the propagation vector at widely varying angles. A similar phenomenon has been observed by Crampin (1967) for second modes along many continental paths crossing Asia.

The behaviour of second modes is particularly sensitive to features of the upper mantle as more than 75 per cent of the energy, at the usually recorded frequencies, travels in the top 30 km of the upper mantle. However, long, large-amplitude second mode wave trains are infrequently recorded, mainly due to the need for long paths over homogeneous, shield-like regions. The longer wave trains contain much information about the nature of the upper mantle, which we may soon be in a position to interpret.

The consequences of aligned anisotropy in the Earth should be borne in mind when making observations of surface waves. The following are some of the effects most likely to be observed. This list could be extended.

1. Generation of fundamental and higher mode Love waves by underground and atmospheric explosions.

2. Particle motion. Anisotropy may result in considerable departures from the retrograde elliptic and transverse particle motions of Rayleigh and Love waves in isotropic media. Rayleigh-type motion will include some transverse motion, and Love-type motion will include some longitudinal motion.

3. Variation of seismic velocity with direction may alter the shape of the dispersion curve as the direction of propagation varies. In particular it is possible for an anisotropic layer to act as a low velocity layer in some directions only.

4. If anisotropy is present, the azimuth of arrival of the wave front is not the same as the azimuth of arrival of the energy. That is to say, the phase velocity does not travel in the same direction as the group velocity.

For directions of propagation having elastic symmetry, the effects listed above will be modified, and the motion will show more similarities with the Rayleigh and Love wave propagation of purely isotropic structures.

Acknowledgments

This work was undertaken as a co-operative project between the Institute of Geological Sciences and the Edinburgh Regional Computing Centre. One of the authors (S.C.) is indebted to the Director of the I.G.S. for permission to publish this paper.

Stuart Crampin:
Institute of Geological Sciences,
Global Seismology Unit,
Edinburgh.

David B. Taylor:
Edinburgh Regional Computing Centre,
Edinburgh.

References

Burridge, R., 1970. The direction in which Rayleigh waves may be propagated on crystals *Q.J. mech. appl. Math.*, **23,** 218–224.

Crampin, S., 1967. Coupled Rayleigh-Love second modes, *Geophys. J. R. astr. Soc.*, **12,** 229–235.

Crampin, S., 1970. The dispersion of surface waves in multilayered anisotropic media, *Geophys. J.R. astr. Soc.*, **21,** 387–402.

Haskell, N. A., 1953. The dispersion of surface waves on multilayered media, *Bull. seism. Soc. Am.*, **43,** 17–34.

Richter, C. F., 1958. *Elementary Seismology*, W. H. Freeman & Co., 768.

Stoneley, R., 1963. The propagation of surface wave in an elastic media, with orthorhombic symmetry, *Geophys. J.R. astr. Soc.*, **8,** 176–186.

Verma, R. K., 1960. Elasticity of some high density crystals, *J. geophys. Res.*, **65,** 757–766.